

Finite Element Analysis for Grooved Dry Friction Clutch

¹Oday I. Abdullah, ²Josef Schlattmann

Institute of Laser and System Technologies, Technical University Hamburg-Harburg, Germany

Email: oday.abdullah@tu-harburg.de

Abstract – A finite element technique has been used to study the effect of radial and /or circumferential grooves (classic models) on the temperature distribution for dry friction clutch during a single engagement. Three-dimensional transient simulations are conducted to study the thermoplastic coupling of the problem. The friction clutch has been discretized using 20-noded brick elements. The effect of the groove area ratio (G.R=groove area /total contact area), number of grooves and their location are investigated. Furthermore, new groove shapes have been suggested, e.g., curved groove. The response of the new suggested groove has been compared to the already existing shapes. The numerical results show that the average temperature of friction material can be controlled by the groove area ratio and shape of the groove. They show as well that the suggested groove improves the response of the friction clutch considerably.

Keywords – Dry friction clutch; Frictional heating; Frictional material; Heat transfer; Temperature field; 3D FEM.

1. Introduction

Automobile friction clutch is an essential component

That most failures and damages in the friction clutch occur due to excessive frictional heat and heat fluctuations. These situations lead to generate high thermal stresses, which causes cracks and deformation for the friction material of clutch. Finally, these disadvantages lead to reduce the lifecycle of the friction material. To prevent the clutch failure before expected lifecycle, it is necessary to know the values of maximum temperature and average temperature and how these depend on known loading condition, physical properties, dimensions of the clutch plates and the degree of air cooling.

Newcomb [1] derived equations of motion during the slipping period, the energy dissipated and the temperature reached at any instant during a single engagement for the clutch when the torque capacity is a function of time. Two typical torque-time variations were discussed and a comparison was made with the case when the torque is assumed to be constant.

The finite difference method used to setting up equations to express the heat balance at every region in the clutch. He determines the temperatures at various elements when band contact occurs between the rubbing surfaces during the operation of an automotive clutch. Temperatures distributions are determined for contact area of different band width on the two clutch facing. Both single and repeated engagements made at regular interval are considered [2].

Newcomb [3] presented expressions to determine the torque capacity of a clutch and the rate of heat dissipated by dry friction during a single clutch engagement, together with equations to enable calculation of the rubbing-path temperatures as well as temperatures at various depths inside the contacting bodies during the slipping period. It was shown how the maximum friction surface temperature varies with the thickness of pressure plate and for design purpose a rapid method of calculating temperatures is given when the slipping time is known.

Yong [4] developed a three-dimension finite volume method to predict the transient thermal response of wet clutch discs during engagement. Unstructured brick or wedge elements were used to represent the geometry so that complex groove patterns could be modelled in a relatively simple manner. The sliding between discs was incorporated through a source / sink term derived from a Lagrangian approach. Furthermore, the heat transfer across different materials was solved together in an implicit manner through the use of a conjugate heat-transfer algorithm. Finally, the method was applied to evaluate the thermal effectiveness of double-parallel and radial groove designs for the same clutch and under the same operating conditions. It was found that the double-parallel groove design was superior to the radial groove design as far as thermal performance is concerned.

Kennedy and Traiviratana [5] used finite element method to study transient heat conduction in two bodies sliding over each other with frictional heat generated at the contact interface. Temperature profiles and heat partition distributions are determined for three cases: two-dimensional conduction between two semi-infinite

sliding bodies in contact over an infinite strip, three-dimensional conduction between two semi-infinite sliding bodies in contact over a square area, and two-dimensional conduction between a sliding railcar wheel and the rail.

[6] developed a two-dimensional finite element model to determine the non-linear steady-state configuration of a two-dimensional thermoelastic system involving sliding in the plane with frictional heat generation. Above a certain critical speed, this causes the uniform pressure solution to be unstable and the final steady-state configuration involves regions of separation at the interface and associated temperature and displacement fields that migrate over the contacting bodies in the direction of sliding. Also, they presented new algorithm to determine this migration speed by iteration to be able to use a reference frame in which the fields are stationary.

[7] simulated the engagement of wet clutches using Berger's model and torque equations. They studied a surface roughness, fluid viscosity, friction characteristics, material permeability, moment of inertia, groove area ratio and Young's modulus. One big concern for the wet clutch engagement is engagement time which affects the friction generated heat and thus the temperature. Another major concern is the torque response that is of importance to study clutch shudder. Surface roughness, viscosity and friction curves affect the engagement time and torque response. The moment of inertia has a big influence on the engagement time rather than the torque. Permeability, groove area and Young's modulus have less effect on the torque than the other parameters.

[8] carried out a numerical simulation to examine the effect of radial and circumferential grooves on the frictional surface temperature and torque response in a multidisc wet clutch. The modified Reynolds equation for hydrodynamic lubrication and heat conduction equation for heat transfer were solved by SOR and ADI methods, respectively. The contact pressure was assumed proportional to the real contact area. The simulation results show that grooving enhances the torque response and the temperature at the surface material can be better controlled by the simultaneous use of radial and circumferential grooving.

[9] used finite element method finite element for dry ceramic clutch disk to find the thermal behavior and comparison with experimental measurement results. In this study the heat partition factor and heat convection coefficient changing in time and space. A distributed heat source was applied for modeling heat generation. The thermal results are in good agreement with the measured temperature.

[10] investigated the effect of radial grooves and waffle-shape grooves on the performance of a wet clutch. Three-dimensional formulation of the governing equations, boundary conditions, and numerical solution scheme are presented for modeling the thermal aspects of the engagement process in a wet clutch. The thermal model includes full consideration of the viscous heat dissipation in the fluid as well as heat transfer into the separator, the friction material, and the core disk. The convective terms in the energy equations for the oil as well as the heat conduction equations in the bounding

solids are properly formulated to determine the temperature fields corresponding to the domains between grooves. Roughness, centrifugal force, deformability, and permeability of the friction material with grooves are taken into account. The effects of groove geometry such as groove depth, grooved area, and number of grooves on the engagement characteristic of a wet clutch are investigated. It is also shown that the thermal effects in a wet clutch influence the engagement time and the torque response.

The aim of this research is to shed light on the importance of grooves in friction clutch, and the effect of these grooves on temperature field for friction material of clutch. Two kinds of grooves models presented in this paper, classic groove models (radial, circumferential and radial with circumferential together) and proposed groove models (curved grooves).

2. Statement of the Problem

The large amount of the kinetic energy is transferred into thermal energy during slipping period (t_s). In this work, it will be assume that all the friction energy consumption due to slipping is transformed into heat energy, which is distributed in the friction interface. Then, the total heat generated during the slipping is given as follows [11],

$$Q_t(r,t) = \mu p V_s; \quad 0 \leq t \leq t_s \quad (1)$$

Where, $V_s = \omega_s r$

And, V_s is the sliding velocity and ω_s is the sliding angular velocity (rad/sec). Assume the sliding angular velocity decreases linearly with time as,

$$\omega_s(t) = \omega_o \left(1 - \frac{t}{t_s}\right), \quad 0 \leq t \leq t_s \quad (2)$$

Where ω_o is the initial sliding angular velocity when the clutch starts to slip ($t=0$).

The heat flux on the clutch surfaces at any time of slipping is,

$$Q_c(r,t) = f_c \mu p r \omega_o \left(1 - \frac{t}{t_s}\right); \quad 0 \leq t \leq t_s \quad (3)$$

Where f_c is the heat partition ratio witch imposes division of heat entering the clutch, pressure plate and flywheel (assume the same material properties for the flywheel and pressure plate), and is given as follows [12].

$$f_c = \frac{\sqrt{K_c \rho_c c_c}}{\sqrt{K_c \rho_c c_c} + \sqrt{K_f \rho_f c_f}} = \frac{\sqrt{K_c \rho_c c_c}}{\sqrt{K_c \rho_c c_c} + \sqrt{K_p \rho_p c_p}} \quad (4)$$

Where k is the thermal conductivity, ρ is the density and c is the specific heat. All values and parameters, which refer to the axial cushion, friction material, flywheel and pressure plate in the following considerations, will have bottom indexes cu , c , f and p respectively.

When the engagement process starts for clutch, the heat will generated between the surfaces due to the slipping (result of the difference in velocities between the driving shaft and driven shaft). The heat generated will dissipate by the conduction between friction clutch components and by convection to environment. Due to short time for slipping process the radiation is neglected. It can be obtained, that the temperature distribution by building three-dimensional models to present the frictional heating process for friction clutch.

The starting point for the analysis of the temperature field in the friction clutch is the parabolic heat conduction equation in the cylindrical coordinate system $\{r$ -radial coordinate (m), θ -circumferential coordinate (rad), z -axial coordinate (m) $\}$, which is centered in the axis of the disc and z points to it's thickness (Fig. 1-a).

$$\frac{\partial^2 T}{\partial r^2} + \frac{1}{r} \frac{\partial T}{\partial r} + \frac{1}{r^2} \frac{\partial^2 T}{\partial \theta^2} + \frac{\partial^2 T}{\partial z^2} = \frac{1}{\alpha} \frac{\partial T}{\partial t}; \quad (5)$$

$$r_i \leq r \leq r_o, 0 \leq \theta \leq 2\pi, 0 \leq z \leq \delta, t > 0$$

Where α is the thermal diffusivity, $\alpha = k/\rho c$

Taking the symmetry of a problem into account, the first step takes symmetry in the circumference direction, this symmetry depends on the configuration of groove in clutch (takes quarter from whole model for all cases). And the second symmetry of a problem is depend on the applied load and boundary conditions (In this work the same value of applied load and same heat transfer coefficient on friction clutch surfaces), this means that the temperature of the solid is symmetric about axial plane in z -axis, that bisects the total thickness of the clutch (thickness of friction material both sides and thickness of axial cushion). On the exposed surfaces of the friction clutch models, the convection takes place with the heat transfer coefficient independent of the temperature. It is also assumed that the material properties of the friction material, flywheel, pressure plate and axial cushion are isotropic and independent of the temperature. Considering the assumptions mentioned above, it's shall find the temperature fields in the clutch from the solution of the following three-dimensional boundary-value problems. The boundary conditions and initial conditions for friction clutch without grooves (Fig. 1-a),

$$K_{cu} \frac{\partial T}{\partial r} \Big|_{r=r_o} = h[T(r_o, z, t) - T_a]; \quad (6)$$

$$0 \leq \theta \leq 2\pi, 0 \leq z \leq t_{cu}/2, t \geq 0$$

Where T_a is the ambient temperature and h is the convection heat transfer coefficient.

$$K_c \frac{\partial T}{\partial r} \Big|_{r=r_o} = h[T(r_o, z, t) - T_a]; \quad (7)$$

$$0 \leq \theta \leq 2\pi, (t_{cu}/2) \leq z \leq (t_{cu}/2) + t_c, t \geq 0$$

$$K_c \frac{\partial T}{\partial z} \Big|_{z=(t_{cu}/2)+t_c} = Q_c(r, t); \quad (8)$$

$$r_i \leq r \leq r_o, 0 \leq \theta \leq 2\pi, 0 \leq t \leq t_s$$

$$K_c \frac{\partial T}{\partial r} \Big|_{r=r_i} = h[T(r_i, z, t) - T_a]; \quad (9)$$

$$0 \leq \theta \leq 2\pi, (t_{cu}/2) \leq z \leq (t_{cu}/2) + t_c, t \geq 0$$

The initial temperature is,

$$T(r, \theta, z, 0) = T_i; \quad (10)$$

$$r_i \leq r \leq r_o, 0 \leq \theta \leq 2\pi, 0 \leq z \leq t_c + (t_{cu}/2)$$

$$\frac{\partial T}{\partial r} \Big|_{r=r_i} = 0; \quad 0 \leq z \leq (t_{cu}/2), t \geq 0 \quad (11)$$

$$\frac{\partial T}{\partial z} \Big|_{z=0} = 0; \quad r_i \leq r \leq r_o, 0 \leq \theta \leq 2\pi, t \geq 0 \quad (12)$$

New condition is added when there is a groove in the surface area of the friction clutch disc (Fig. 1-b),

$$Q_{conv} = h[T(r, z, t) - T_a]; \quad t \geq 0 \quad (13)$$

Where Q_{conv} is the rate of convection heat transfer for grooves areas.

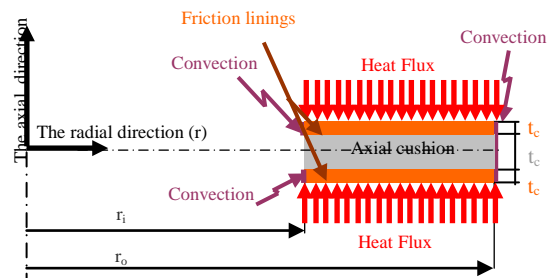
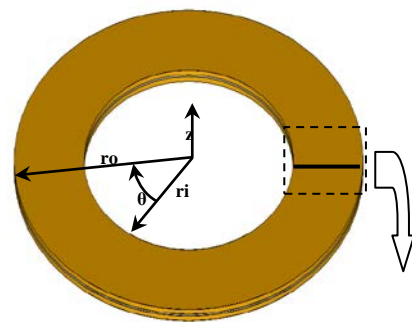


Fig. 1.a The boundary conditions of the friction clutch disc (Without groove)

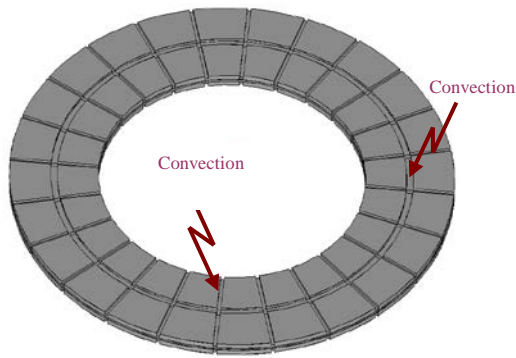


Fig. 1.b The boundary conditions of the friction clutch disc (With groove)

3. Finite Element Formulation

Transient condition involved time dependent function of the heat transfer analysis. Cook [13] stated that in transient condition, temperature change in a unit volume of material is resisted by thermal mass that depends on the mass density ρ of the material and its specific heat c . He stated that for transient condition, the finite element formulation can be expressed as,

$$[C]\{\dot{T}\} + [K]\{T\} = \{F\} \quad (14)$$

Where, $[C]$ is the specific heat matrix, $[K]$ the conductivity matrix, $\{T\}$ the vector of nodal temperatures, $\{\dot{T}\}$ is the derivative of temperature with time ($\dot{T} = \partial T / \partial t$), and $\{F\}$ the applied heat flows. In order to determine temperature distribution of this transient heat conduction problem, the fine mesh element was essential. Moreover, when the iterative method of the given problem is employed, then a relatively short time is needed for the calculations. In the next step of the study, the Crank-Nicolson method was selected as an unconditionally stable scheme. In this paper ANSYS software was used to investigate transient thermoelastic analysis behavior of dry friction clutch. Two types of loads are applied in this paper (Fig. 2); the first load type is the uniform pressure (load type A) and the second load type is the uniform wear (load type B). In all computations for the friction clutch model, it has been assumed a homogeneous and isotropic material and all parameters and materials properties are listed in Table I.

The heat transfer coefficient has been taken as 40.89 W/m² K [2] and is assumed to be constant over all exposed surfaces, and the slipping time is 0.4 s. Fig. 3 shows the three dimensional models of friction clutches for the classic groove models (radial, circumferential and, radial and circumferential) and proposed groove model (curved). The twenty-noded thermal element (SOLID90) was used in this analysis; the element has one

temperature degree of freedom at each node as the temperature is scalar. Also these elements have compatible temperature shapes and are well suited to model curved boundaries. A mesh sensitivity study was done to choose the optimum mesh from computational accuracy point of view.

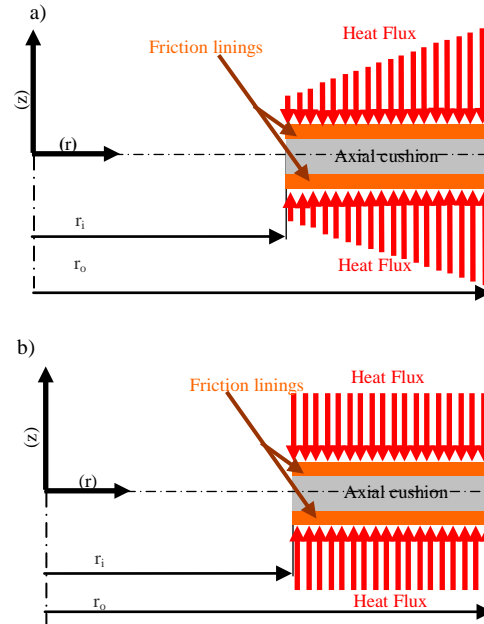


Fig. 2 Thermal load (during the slipping) on the friction material surfaces of the clutch (a) Type A. (b) Type B.

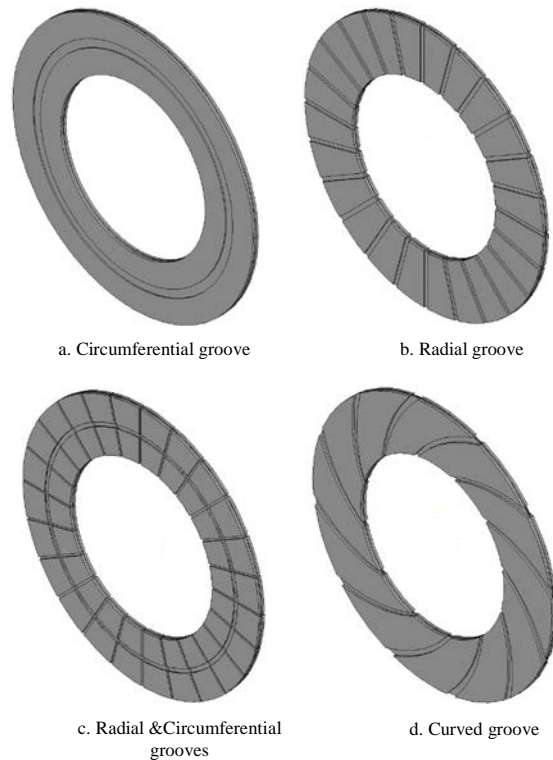


Fig. 3 the grooves models for friction clutches

Thermophysical Properties of Materials and Operations
Conditions for the Thermal Analysis

Table. 1 Thermomechanical properties of materials and operators conditions for the thermal analysis

| | |
|---|--------|
| Inner radius, r_i [m] | 0.093 |
| Outer radius, r_o [m] | 0.155 |
| Thickness of friction material, t_c [m] | 0.0028 |
| Thickness of the axial cushion, t_{cu} [m] | 0.0012 |
| Depth of the grooves, [m] | 0.0005 |
| Maximum pressure for Type A, p_{max} [MPa] | 0.73 |
| Maximum pressure for Type B, p_{max} [MPa] | 1 |
| Coefficient of friction, μ | 0.3 |
| Number of friction surfaces, n | 2 |
| Maximum angular slipping speed, ω_o (rad/sec) | 194 |
| Conductivity for friction material, K_c (W/mK) | 0.75 |
| Conductivity for pressure plate & flywheel, K_p & K_f (W/mK) | 56 |
| Density for friction material, ρ_c (kg/m ³) | 1000 |
| Density for pressure plate & flywheel, ρ_p & ρ_f (kg/m ³) | 7200 |
| Specific heat for friction material, c_c (J/kgK) | 1400 |
| Specific heat for pressure plate & flywheel, c_p & c_f (J/kgK) | 450 |
| Time step, Δt (s) | 0.0005 |

4. Results and Discussions

Series of computations have been carried out using ANSYS software to study the effect of grooves (classic and proposed models) on the temperature distribution for dry friction clutch during a single engagement.

Fig. 4 and 5 show the contour of temperature distribution for friction material surface for all models of grooves (radial, circumferential, radial & circumferential and curved) at time 0.2 s for type A and type B respectively. It can be seen, for the load type A the temperature grows from minimum value at the inner radius to maximum value at the outer radius, and for the load type B is approximately uniform temperature on the surfaces. The values of the maximum temperature for load type A (uniform pressure) are greater than load type B (uniform wear), these result because of the thermal load function for type A grows as a function of radius (start from minimum value of load at inner radius to maximum load value at the outer radius, and the maximum load for load type A is greater than the load in type B), and for load type B the thermal load is constant with radius. Also, it is seen that the difference in the values of maximum temperatures between all models under the same conditions is neglected.

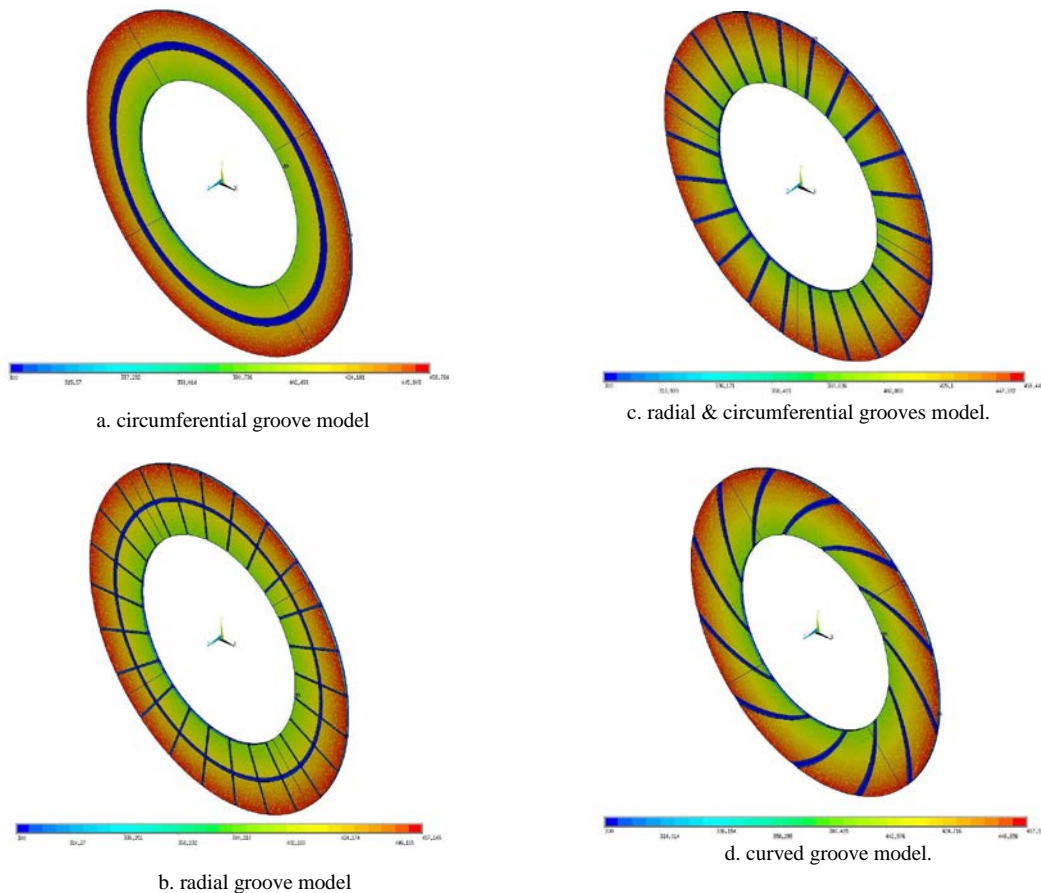


Fig. 4 The temperature distribution [k] at t=0.2 S (Type A, G.R=0.12)

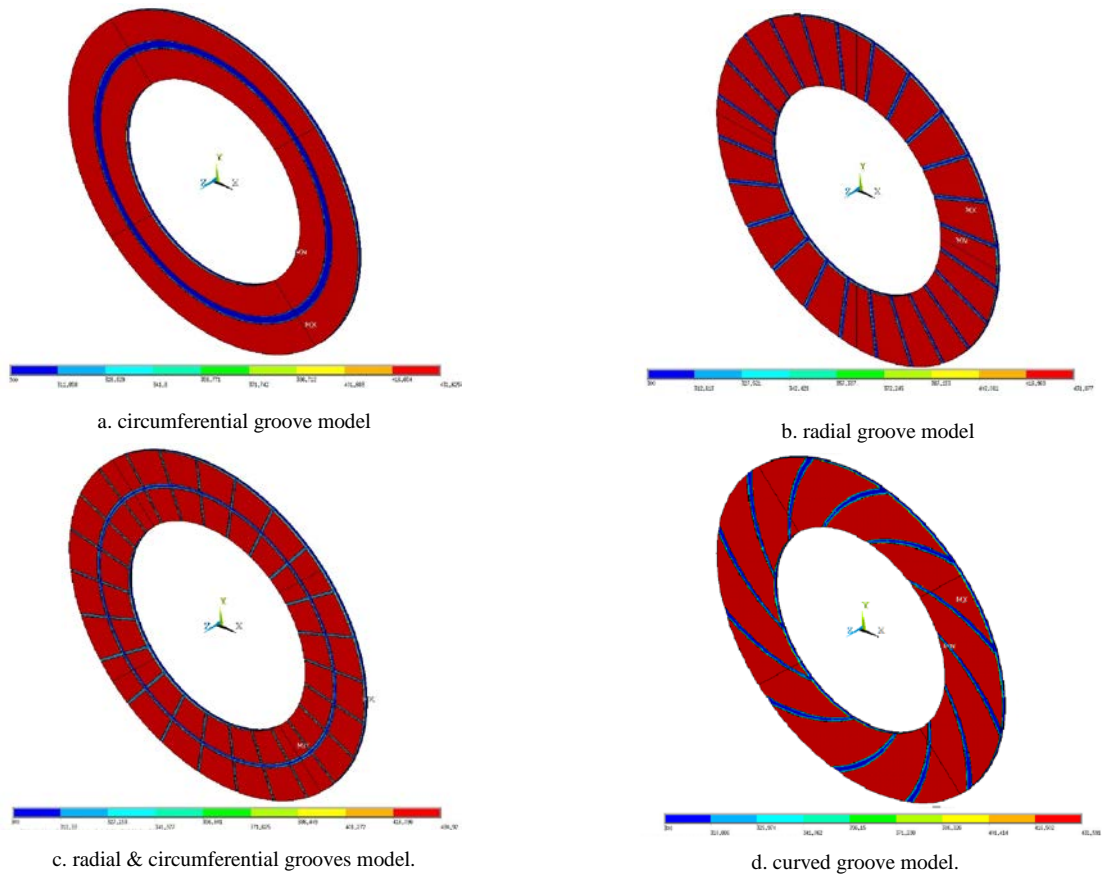


Fig. 5 The temperature distribution [k] at $t=0.2$ s (Type B, G.R=0.12)

Figs. 6 & 7 present the variation of temperature distribution with friction material thickness (z) for different time step (load type A). It can be seen from these figures, that the maximum effect of temperature occur at outer radius and at the contact surface ($z=3.4$ mm), and then the effect of load decreases with thickness to zero approximately at mid point of thickness of the friction material ($z=2$ mm) for inner and outer radius. The maximum difference in the temperature between the inner and outer radius occurs at ($z=3.4$ mm) and 0.2 s is 60.29 K.

Figs. 8 & 9 show the variation of temperature with (z) for different time step (load type B). It can be seen from these figures that the small difference in temperatures between inner and outer radius and the same behavior of Figs. 5 & 6 for temperature with (z), the maximum effect of thermal load occur at the surface and then decreases to zero at the mid point of friction material thickness. The maximum difference in the temperature between the inner and outer radius occurs at ($z=2.84$ mm) and 0.2 s is 6.1 K.

Figs. 10 & 11 show the variation of temperature with time for different locations at the surface for type A and type B respectively. It can be noted, that the values of temperature for load A start from minimum values of temperature at inner radius to maximum values of temperatures at outer radius, and for type B the different behavior, the minimum values of temperature occur at inner radius and then the temperature increases to maximum near the middle point between the inner and outer radius ($r=0.124$ m) and finally the temperature decreases at outer radius, but also here the values of temperatures at outer radius are greater than the temperature values at inner radius. The maximum difference in the temperature between the inner and outer radius are 63.424K at 0.18s for load type A and 14.326 K at 0.0575 s for load B.

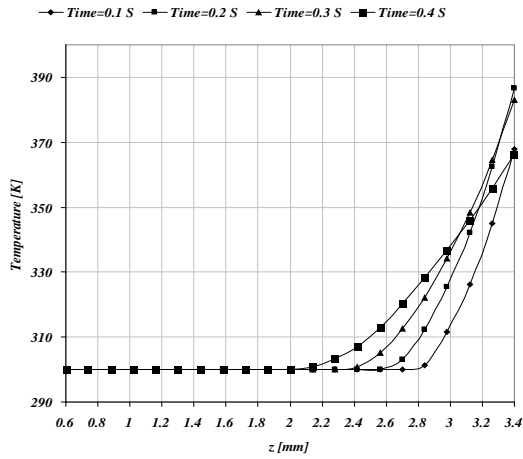


Fig. 6 Variation of temperature at inner radius with thickness (G.R=0, Type A)

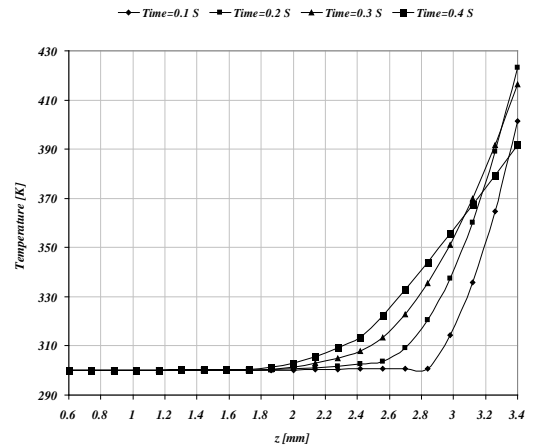


Fig. 9 Variation of temperature for at outer radius with thickness (G.R=0, Type B)

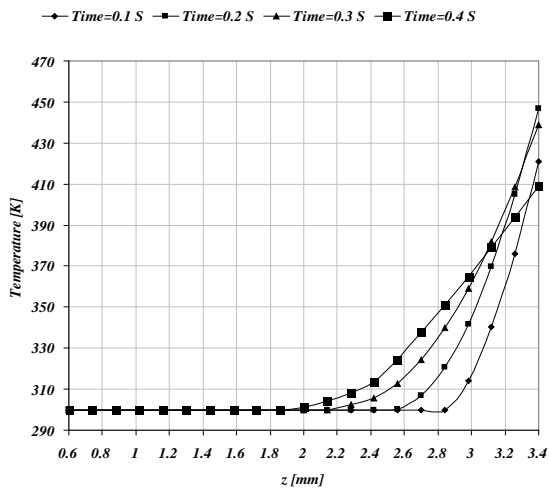


Fig. 7 Variation of temperature at outer radius with thickness (G.R=0, Type A)

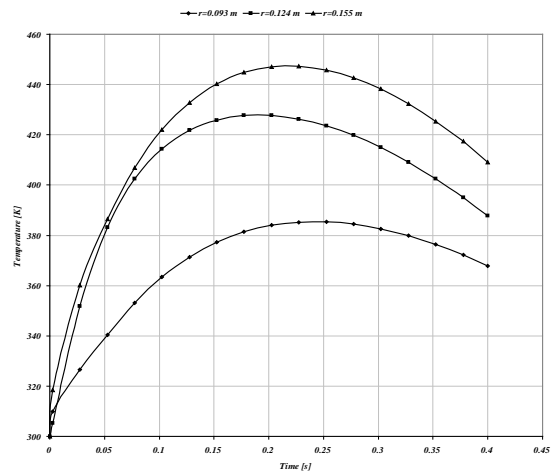


Fig. 10 Variation of temperature for different radius with time (G.R=0, Type A)

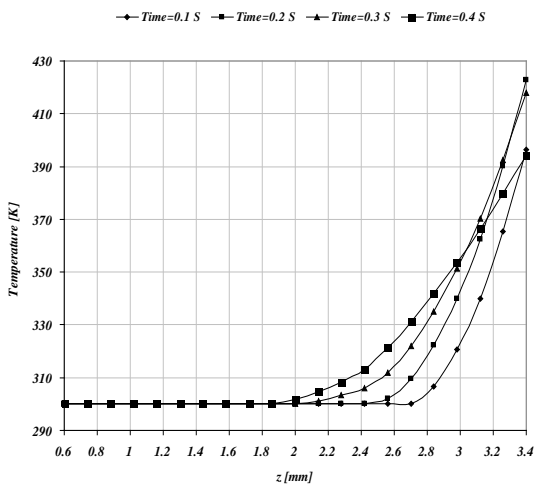


Fig. 8 Variation of temperature at inner radius with thickness (G.R=0, Type B)

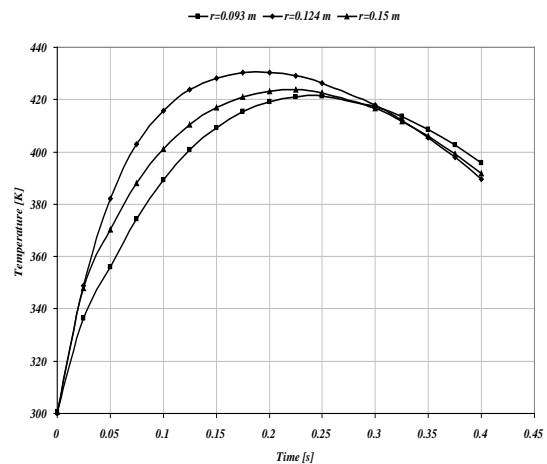


Fig. 11 Variation of temperature for different radius with time (G.R=0, Type B)

For the load type A, Figs. 12, 13 & 14 demonstrate the variations of maximum temperature for different groove area ratio with time for the classic grooves models (circumferential, radial, radial & circumferential grooves), and for type B Figs. 15, 16 & 17 show the maximum temperature with time for the same models. In all figures, it's observed that the temperature increases from initial temperature at ($t_s=0$) to maximum values approximately at $t_s=0.2$ (near the half time of slipping) then decreases at the end. The maximum temperature difference ($T_{max}-T_i$) at $t_s=0.2$ s are found (157 K and 133 K) corresponding to the type A and type B respectively.

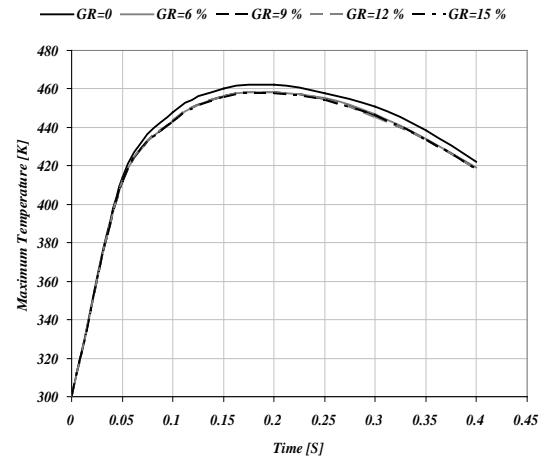


Fig. 14 Variation of maximum temperature for different groove area ratio with time (radial & circumferential grooves model, Type A)

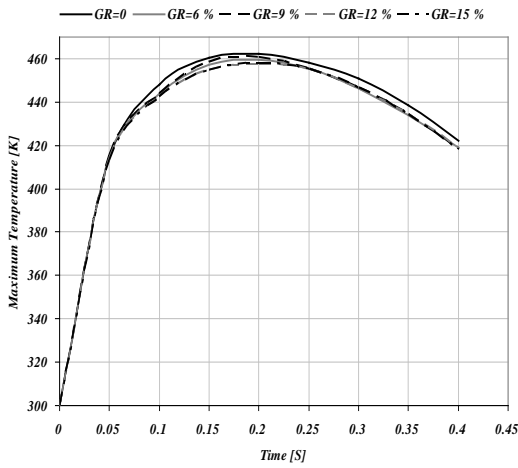


Fig. 12 Variation of maximum temperature for different groove area ratio with time (circumferential groove model, Type A)

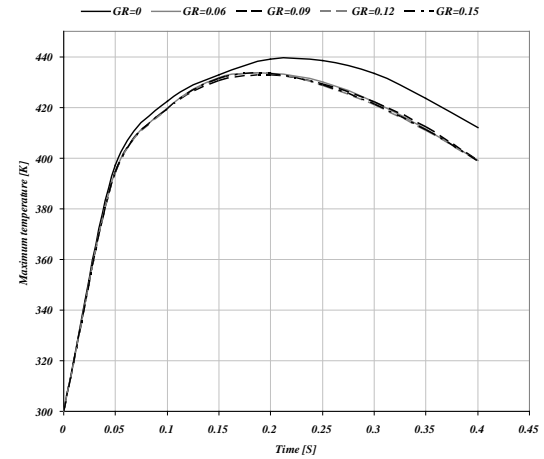


Fig. 15 Variation of maximum temperature for different groove area ratio with time (circumferential groove model, Type B)

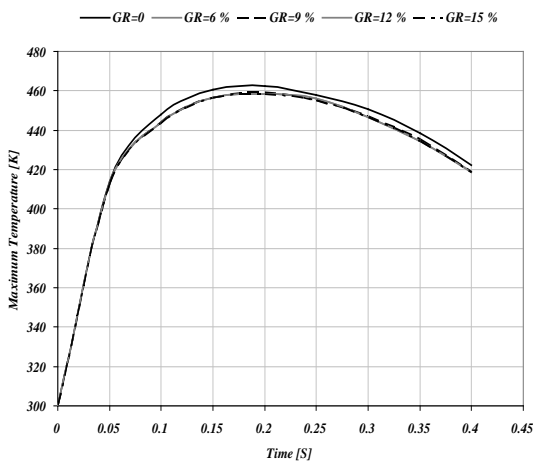


Fig. 13 Variation of maximum temperature for different groove area ratio with time (radial groove model, Type A)

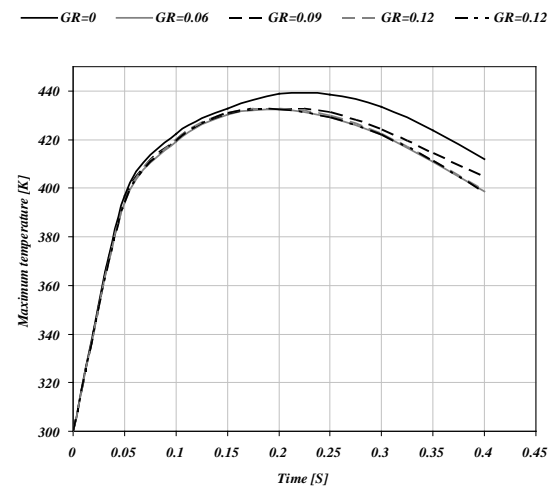


Fig. 16 Variation of maximum temperature for different groove area ratio with time (radial groove model, Type B)

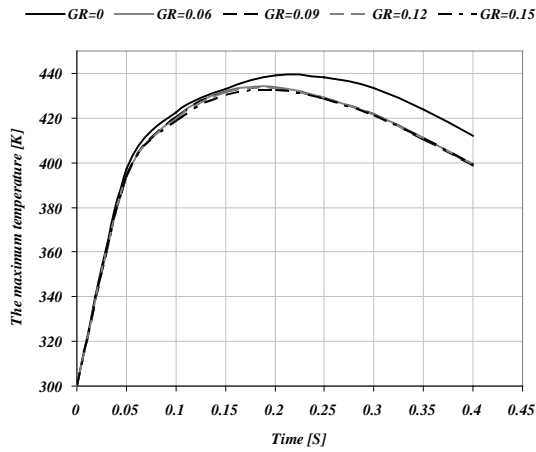


Fig. 17 Variation of maximum temperature for different groove area ratio with time (Radial & circumferential grooves model, Type B)

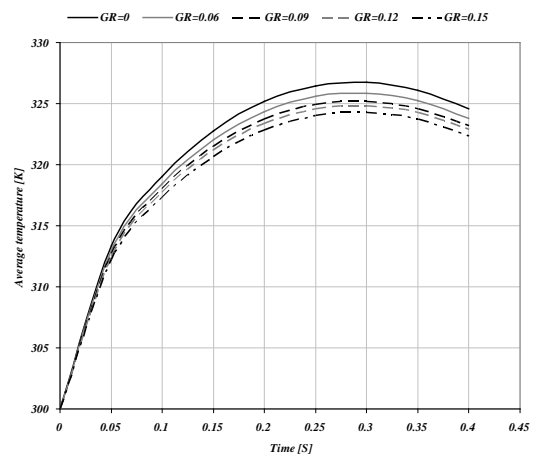


Fig. 19 Variation of average temperature for different groove area ratio with time (circumferential groove model, Type B)

Figs. 18, 19, 20, 21, 22 & 23 display the variations of the average temperature for different groove area ratios and different groove models (circumferential, radial, radial & circumferential) with time for loads type A and type B. It can be detected in these figures, that the maximum values of the average temperature occur at $t_s=0.3$. The maximum difference in the average temperature between the friction material with groove and without groove occurs when used the circumferential groove model are 2.769 K and 2.46 K at 0.3s for G.R=0.15 corresponding to load type A and type B respectively.

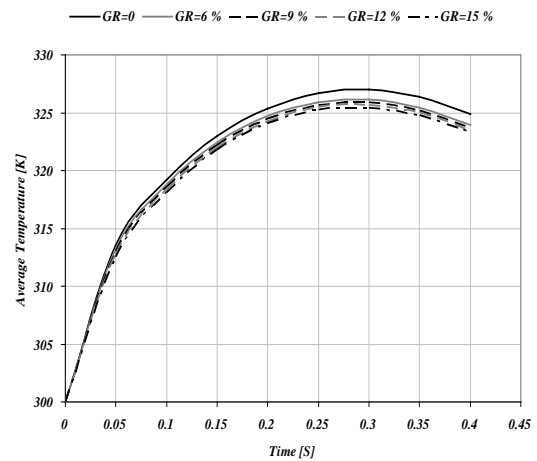


Fig. 20 Variation of average temperature for different groove area ratio with time (radial groove model, Type A)

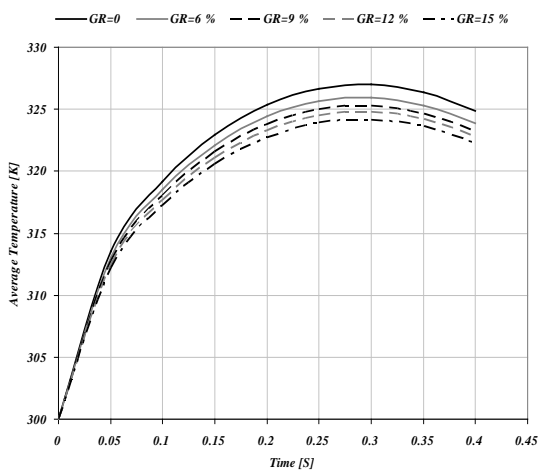


Fig. 18 Variation of average temperature for different groove area ratio with time (circumferential groove model, Type A)

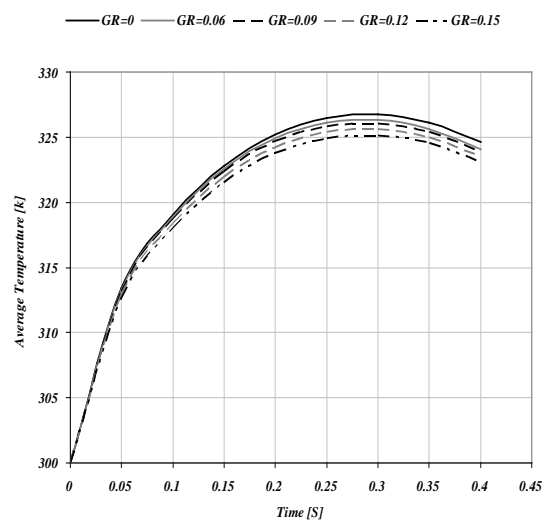


Fig. 21 Variation of average temperature for different groove area ratio with time (radial groove model, Type B)

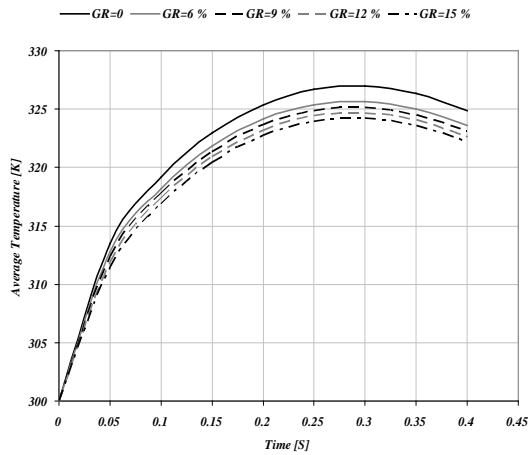


Fig. 22 Variation of average temperature for different groove area ratio with time (radial & circumferential grooves model, Type A)

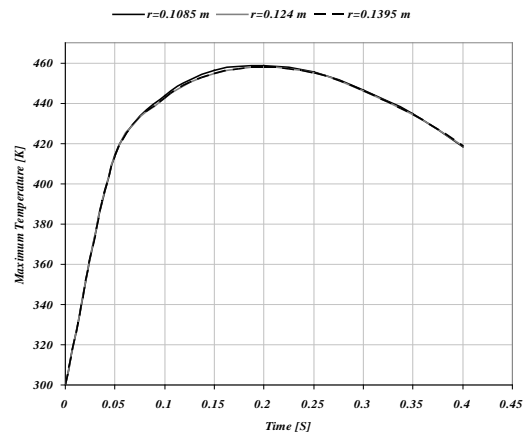


Fig. 24 Variation of maximum temperature for different location of groove with time (circumferential groove model, G.R=0.12, Type A)

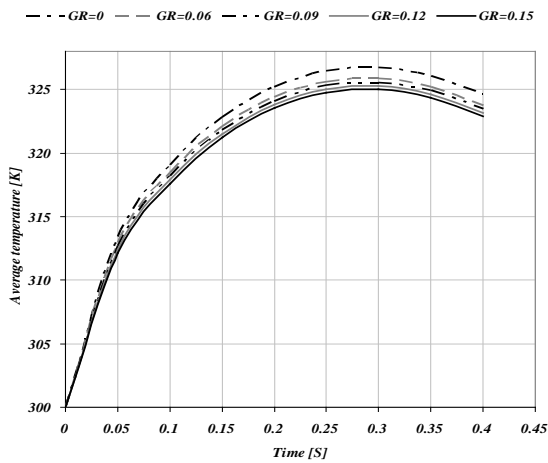


Fig. 23 Variation of average temperature for different groove area ratio with time (Radial & circumferential grooves model, Type B)

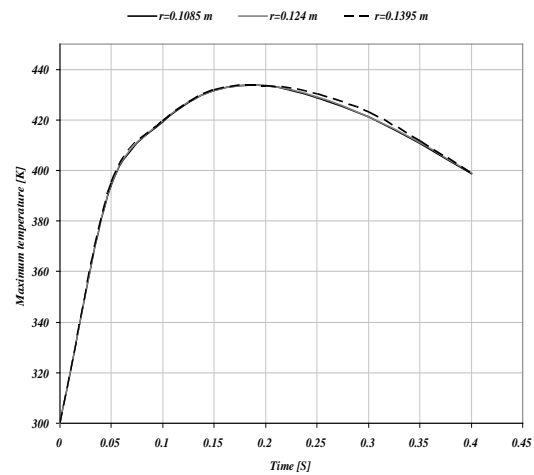


Fig. 25 Variation of maximum temperature for different location of groove with time (circumferential groove model, G.R=0.12, Type B)

Figs. 24 & 25 show the variations of the maximum temperature for different location of circumferential groove with time for load type A and type B respectively (G.R=0.12). It can be noted from these figures, there is no effect of groove location on the values of the maximum temperature.

Figs. 26 & 27 show the variations of the average temperature for different location of circumferential groove with time for load type A and type B respectively (G.R=0.12). It can be observed, that the minimum values of average temperatures occur at mid point between inner and outer radius ($r=0.124$ m) for type A, but for type B occur at ($r=0.1085$ m).

Figs. 28, 29, 30 and 31 show the variations of maximum temperature and average temperature for different numbers of groove of circumferential groove model with time for load type A and type B (G.R=0.12). It can be noted from these figures, there is no effect of number of grooves on the maximum and average temperatures under the same conditions.

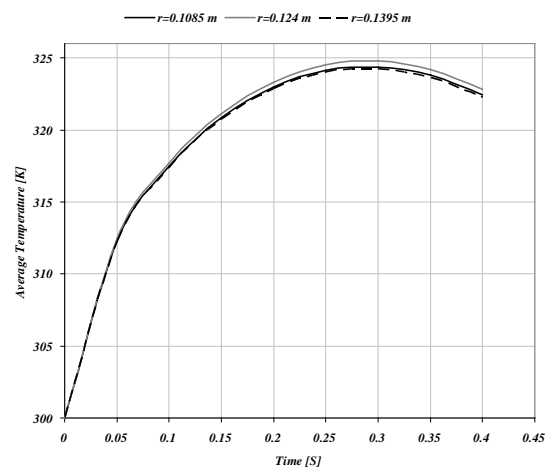


Fig. 26 Variation of average temperature for different location of groove with time (circumferential groove model, G.R=0.12, Type A)

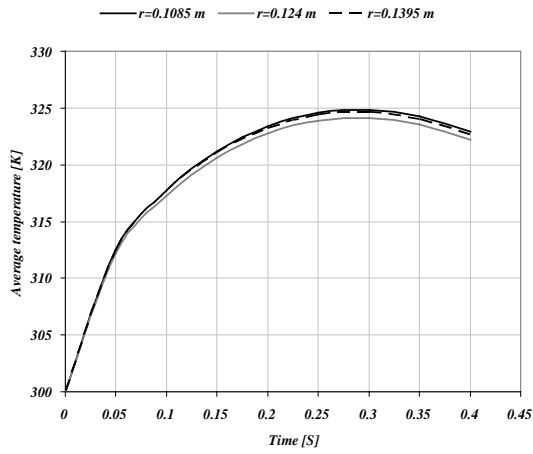


Fig. 27 Variation of average temperature for different location of groove with time (circumferential groove model, G.R=0.12, Type B)

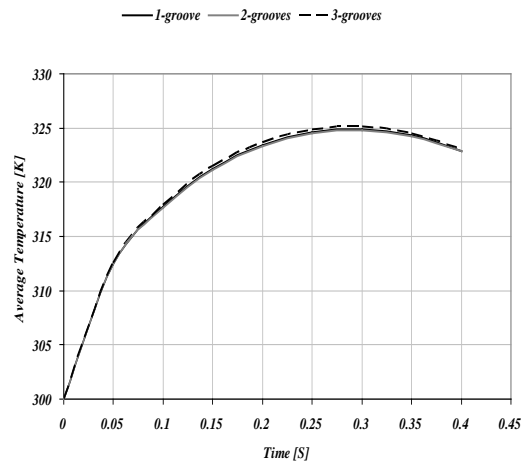


Fig. 30 Variation of average temperature for different number of grooves with time (circumferential groove model, G.R=0.12, Type A)

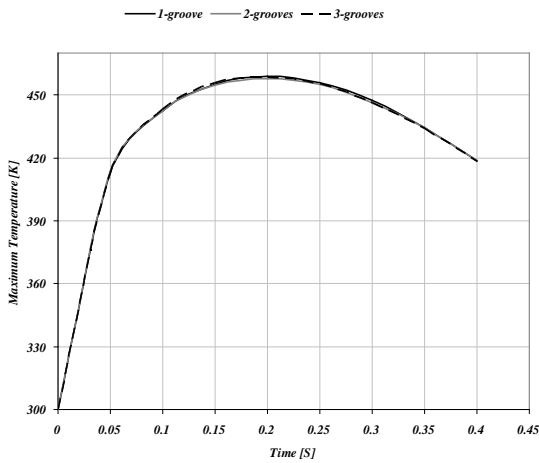


Fig. 28 Variation of maximum temperature for different number of grooves with time (circumferential groove model, G.R=0.12, Type A)

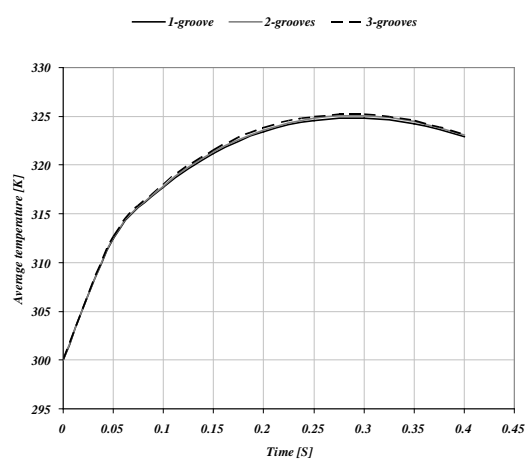


Fig. 31 Variation of average temperature for different number of grooves with time (circumferential groove model, G.R=0.12, Type B)

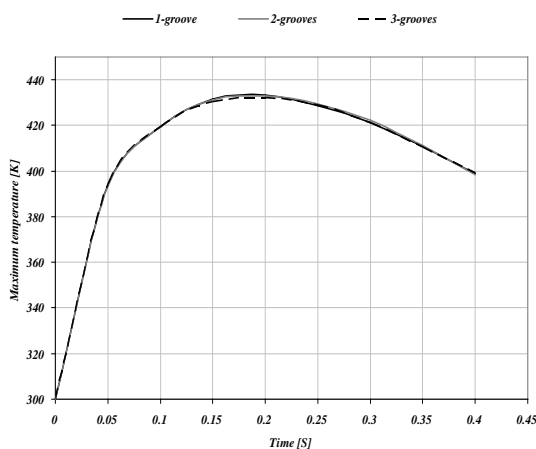


Fig. 29 Variation of maximum temperature for different number of grooves with time (circumferential groove model, G.R=0.12, Type B)

Figs. 32 and 33 demonstrate the variations of maximum temperature for different groove models (classic and proposed) with time for type A and type B respectively (G.R=0.12). It can be noted, there is no effect of groove shape on the maximum temperature under the same boundary conditions.

Figs. 34 and 35 show the variations of average temperature for classic and proposed grooves models with time for loads type A and type B respectively (G.R=0.12). It can be noted, that the lower values of the average temperatures occur when used the curved groove model under the same conditions.

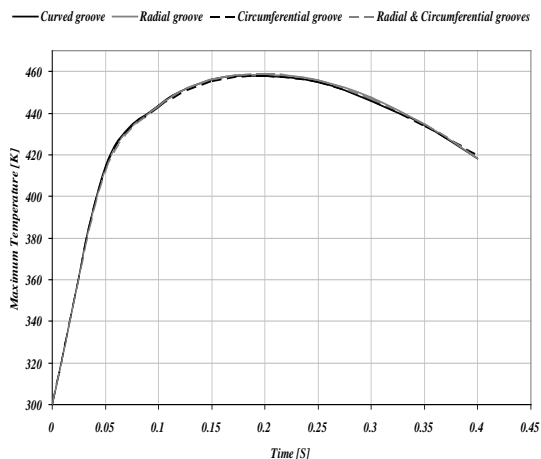


Fig. 32 Variation of maximum temperature for different types of grooves with time (G.R=0.12, Type A)

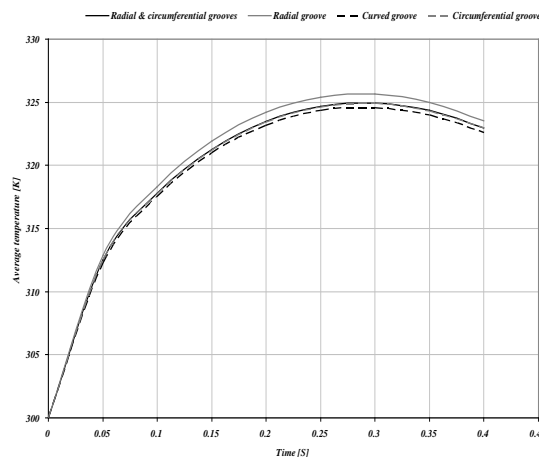


Fig. 35 Variation of average temperature for different types of grooves with time (G.R=0.12, Type B)

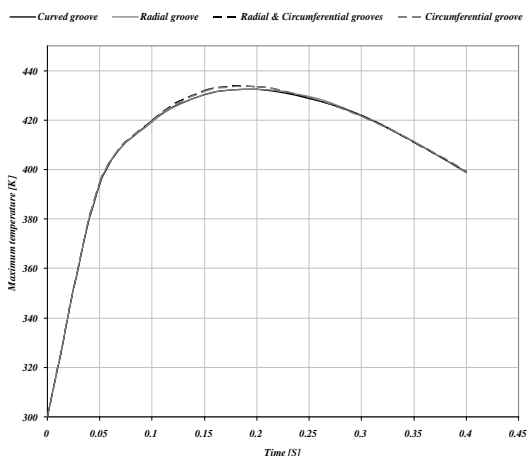


Fig. 33 Variation of maximum temperature for different types of grooves with time (G.R=0.12, Type B)

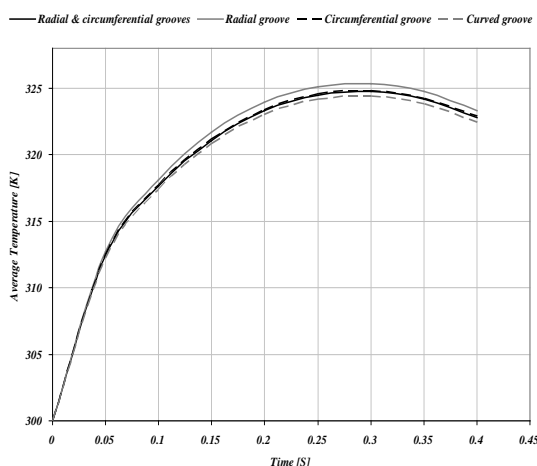


Fig. 34 Variation of average temperature for different types of grooves with time (G.R=0.12, Type A)

5. Concluding Remarks

In this paper transient thermal analysis for the dry friction clutch disc in a single engagement was performed. Three-dimensional model was built to obtain the numerical simulation for parabolic heat transfer equation. The results show that both evolution of sliding speed of disc and contact pressure with specific material properties intensely effect disc clutch temperature fields in the domain of time. Proposed transient FE modeling technique of two types of thermal load (type A: uniform pressure and type B: uniform wear). It can be seen, that the result of temperature distribution for the load type A is more than load type B, because of the total quantity of load A is greater than load type B, and the function of load type A grows as a function of radius (from minimum value of load at inner radius to maximum value at the outer radius), but for load type B the thermal load is constant with radius. The highest values of maximum temperature and average temperature occur approximately at 0.2 s and 0.3s respectively during the slipping process for the period of 0.4 s for both types of thermal load.

The maximum effect of the groove on the maximum temperature occurs for the uniform wear case, and the maximum percentage reduction in the maximum temperature are found 1.1% for load type A (circumferential groove) at $t_s=0.15s$ and 3.3% for load type B (radial groove) at $t_s=0.4s$. From the comparison between the average temperature results for new groove model (curved) and classic groove models (radial, circumferential and radial & circumferential), it can be concluded that the new groove model improves the trend for the average temperature for both types of load. Generally for all types of thermal loads, it can be concluded the maximum effect of load occurs at the surface of contact and the effect decreases with thickness of friction material to zero approximately at mid point of their thickness. The present paper is a preliminary of subsequent investigation of the effect of the grooves on multi-engagement of clutch disc for different contact

areas and material properties, also study the effect of thermoelastic instability on the temperature distribution.

References

- [1] NEWCOMB, T. P, "Calculation of Surface Temperatures Reached in Clutches When the Torque Varies with Time", *J. Mech. Engng. Sci.*, 1961, 3, pp-340.
- [2] M El-sherbiny, T P Newcomb, "Temperature distributions in automotive dry clutches", *Proceedings of the Institution of Mechanical Engineers 1847-1996*, 1976, Vol. 190, pp. 359-365.
- [3] NEWCOMB, T. P, "Temperature Reached in Friction Clutch Transmissions", *J. Mech. Eng. Sci.* 2, pp-273 (1960).
- [4] Yong G. Lai , "Transient Effects On Heat Conduction In Sliding Bodies", *Numerical Heat Transfer, Part A: Applications* 33, pp. 583-597 (1998).
- [5] T. C. Kennedy and S. Traiviratana, "Transient Effects On Heat Conduction In Sliding Bodies", *Numerical Heat Transfer, Part A: Applications* 47, pp. 57-77 (2004).
- [6] E. A. Al-Bahkali & J. R. Barber, "Nonlinear Steady State Solution For A Thermoelastic Sliding System Using Finite Element Method", *J. Thermal Stresses* 29, pp 153-168 (2006).
- [7] Hong Gao & Gary C. Barber, "Engagement of a Rough, Lubricated and Grooved Disk Clutch ith a Porous Deformable Paper-Based Friction Material", *J. Teratology Transactions* 45, pp 464-470 (2002).
- [8] Masatoshi Miyagawa, Masataka Ogawa & Hiroki Hara, 'Numerical Simulation of Temperature and Torque Curve of Miltidisk Wet Clutch with Radial and Circumferential Grooves', *Tribology Online* 4, pp 17-21 (2009).
- [9] Balázs Czél, Károly Váradi, Albert Albers and Michael Mitariu, 'Fe thermal analysis of a ceramic clutch', *Tribology International* 45, pp. 714-723 (2009).
- [10] J. Y. Jang, M. M. Khonsari and Rikard Maki, "Three-Dimensional Thermohydrodynamic Analysis of a Wet Clutch With Consideration of Grooved Friction Surfaces", *J. Tribology* 133 (2011).
- [11] F. F. Ling, "A Quasi-Iterative Method for Computing Interface Temperature Distributions", *Zeitschrift für angewandte Mathematik und Physik (ZAMP)* 10, pp. 461-474 (1959).
- [12] H. Blok, "Fundamental Mechanical Aspects in Boundary Lubrication", *SAE Trans.* 46, pp. 54-68 (1940).
- [13] Robert Cook, "Finite Element Modeling for Stress Analysis", *John Wiley & Sons*, (1995).